Fluid Dynamics Transactions, Vol. 5, Part I, pp. 289–298
Institute of Fundamental Technical Research, Polish Academy of Sci., Warsaw

ON THE STRUCTURE OF SHOCK WAVES IN A BUBBLE-LIQUID MIXTURE

L. VAN WIJNGAARDEN (ENSCHEDE)

In this lecture, I propose to give a short account of our work on shock waves in bubble-liquid mixtures. A more detailed account of the theoretical part of the work can be found in [1].

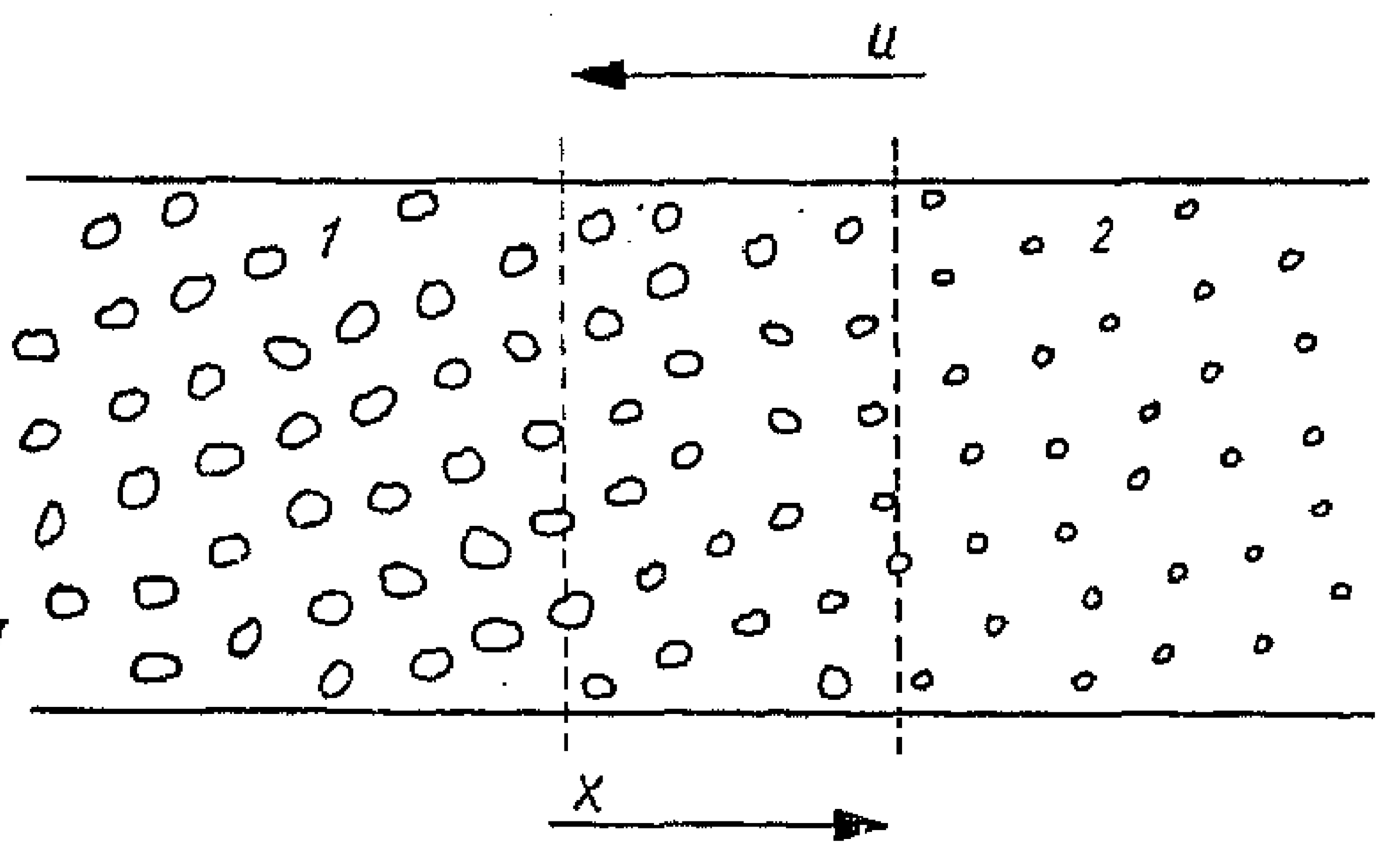

FIG. 1. Shock wave propagation with velocity U from right to left in bubble-liquid mixture.

Since a bubble-liquid mixture is a compressible fluid, shock waves can be generated. This has been demonstrated, e.g., by CAMPBELL and PITCHER [2]. These authors established also the conservation equations analogous to the Hugoniot relations for ordinary shock waves, considering the mixture as a homogeneous fluid.
In particular, if in Fig. 1 the low pressure side of a shock wave is characterized by 1, the high pressure side by 2, they showed that

$$\frac{p_2}{p_1} = \mathsf{M}_1^2. \tag{1}$$

Here the Mach number M_1 expresses the ratio of speed of propagation of the shock wave U to the speed of sound c in the undisturbed region. The latter is (see e.g. [3]) given by

$$c^2 = \frac{p}{\rho_f \beta}, \tag{2}$$

where p denotes pressure, ρ_f the density of the fluid, and β the gas concentration by volume, under the assumption that this is a small quantity,

$$\beta \ll 1. \tag{3}$$

In order to obtain some insight into the structure of the shock wave the dynamic behaviour of the individual bubble must be considered. This is ignored in the homogeneous fluid theory from which not more than relations of the Hugoniot type can be obtained. A difference between local average pressure p and pressure in the bubbles p_g arises due to inertia of the fluid adjacent to an expanding or compressed bubble, and due to viscous stresses in the fluid associated with radial motion. This difference is, with a bubble of radius R, a fluid viscosity μ, given by

$$p_g - p = \rho_f \left\{ R\frac{d^2R}{dt^2} + \frac{3}{2}\left(\frac{dR}{dt}\right)^2 \right\} + \frac{4\mu}{R}\frac{dR}{dt}. \tag{4}$$

The first two terms on the right lead, when incorporated in the dynamics of pressure waves in a bubble-liquid mixture (c. f. [3]), to dispersion of these waves, whence we call these dispersion terms.

Another effect of importance may be (see BATCHELOR [4]) the relative translational motion of the bubbles with respect to the surrounding fluid. When we take as resistance law for the bubbles, moving with velocity v in a fluid with velocity u,

$$K = 12\pi\mu R(v-u),$$

which holds for gas bubbles in a fluid at moderately high Reynolds numbers (see e.g. LANDAU and LIFSHITZ [5], § 45), then it may be shown that the relative velocity $v-u$ is,

$$v-u = 2\int_{-\infty}^{t} \frac{du}{d\tau} e^{-\frac{18\nu}{R^2}(t-\tau)} d\tau. \tag{5}$$

Associated with this relative motion is a Kelvin impulse (see LAMB [6], § 119), given by the relative velocity times the virtual mass of the bubble. Both effects play a role in the mechanism of the shock. To express the conservation of mass and momentum in the mixture, which is assumed to be in isothermal state, we choose a frame of reference moving with the shock. The bubbles have locally radius R, number density n, velocity v, whereas the velocity of the fluid is again denoted by u. Mass density ρ is, neglecting the mass of the gas, given by

$$\rho = \rho_f(1-\beta). \tag{6}$$

Mass conservation requires

$$\rho_f(1-\beta)(u+U) = \rho_f(1-\beta_1)U, \text{ or}$$

$$u = U(\beta-\beta_1). \tag{7}$$

For small β_1, u is small with respect to U so that we may approximate in (3) and other expressions $\frac{d}{dt}$ by $U\frac{d}{dx}$, where x runs along the shock from the low pressure side to the high pressure side. Further, since the total number of bubbles passing a section is conserved—i.e.,

$$(v+U)\,n = \text{constant},$$

and v is of order u — we may take n constant.

The conservation of total momentum, including the Kelvin impulse due to relative motion, requires:

$$\frac{d}{dx}\{\rho_f(1-\beta)(u+U)^2+\tfrac{2}{3}\pi n U R^3(v-u)+p\}=0. \tag{8}$$

The pressure p can be expressed in terms of p_g by (2). For isothermal conditions we have, further

$$p_g=\frac{p_1\,\beta_1}{\beta}. \tag{9}$$

First we disregard the dispersion terms in (2) and take, expressing also R in terms of β and approximating $\frac{d}{dt}$ by $U\frac{d}{dx}$,

$$p=\frac{p_1\beta_1}{\beta}-\frac{4}{3}\frac{\mu U}{\beta}\frac{d\beta}{dx}. \tag{10}$$

Inserting (10) for p, (5) for $v-u$ in (8) leads, taking account of (3) and using (7), after some manipulation to

$$(\beta_1-\beta)(\beta-\beta_2)=-\frac{4}{3}\frac{\nu}{u}\frac{d\beta}{dx}+\beta^2(\beta-\beta_1)+\frac{18\nu}{UR^2}\beta^2\int_{-\infty}^{x}(\beta-\beta_1)\,e^{-\frac{18\nu}{UR^2}(x-\xi)}d\xi. \tag{11}$$

Here, use has been made of the fact that by (1) and (2) the gas contents far upstream and downstream are related through

$$\frac{\beta_1}{\beta_2}=\frac{U^2}{c_1^2}. \tag{12}$$

On the righthand side of Eq. (11) the first term represents the influence of radial relative motion, the two other terms the influence of the translational motion. One of these, $\beta^2(\beta-\beta_1)$, is due to the spreading of momentum by the relative motion of the bubbles On account of (3), this is a small effect with respect to the convection of momentum expressed by the lefthand side of the equation. The remaining term is associated with the dissipation by translational motion. From (11) it follows that the ratio of this with respect to the dissipation by radial motion is, with a shock thickness d, of order

$$\frac{\beta^2 d^2}{R^2}. \tag{13}$$

A first estimate for d can be made by arguing that during the passage of a shock wave, in a time of order d/c, a bubble is reduced in size, which requires a time of order ω_B^{-1} where ω_B is the resonance bubble frequency:

$$\omega_B=\left(\frac{3p}{\rho_f R^2}\right)^{\frac{1}{2}}. \tag{14}$$

Using (2) for c this leads to the estimate

(15) $$d > \frac{R}{\beta^{\frac{1}{3}}}.$$

Using this estimate for d, it follows that the ratio in (13) is a small quantity when (3) holds. We therefore neglect the effect of translational relative motion in what follows, and examine the validity of this afterwards. Upon disregarding of the effects of relative translational motion Eq. (11) can be solved exactly. The solution tending for $x \to -\infty$ to β_1 and for $x \to +\infty$ to β_2 is

(16) $$\beta = \frac{\beta_1+\beta_2}{2} - \frac{\beta_1-\beta_2}{2} \tanh\left\{\frac{3U\beta_1\left(1-\frac{p_1}{p_2}\right)x}{4\nu}\right\}.$$

From this relation a shock thickness of order $\frac{\nu}{U\beta_1(1-(p_1/p_2))}$ follows. For the experimental values given in [1] for U_1, β_1, ν and p_1/p_2, the shock thicknesses calculated from this relation are unrealistically small, since they turn out to be of the same order as or smaller than the bubble size. We next incorporate the inertia terms on the righthand side of (4) in the expression for p in (8). Restricting ourselves to weak shocks and shocks of moderate strength, we linearize the dispersion terms. The second term on the righthand side of (4) is negligible in a linearized approximation, whereas the first one can be written as

(17) $$\frac{\rho_f \bar{R}^2 U^2}{3\bar{\beta}} \frac{d^2\beta}{dx^2},$$

where the quantities with a bar denote those with respect to which linearization is carried out. Always neglecting the effects of relative translational motion, we obtain, in the same way as (11) was obtained from (8), but this time including (17) in the relation between p and p_g:

(18) $$(\beta_1-\beta)(\beta_2-\beta) = \frac{\bar{R}^2}{3}\frac{d^2\beta}{dx^2} + \frac{4}{3}\frac{\nu}{U}\frac{d\beta}{dx}.$$

This equation holds for weak shocks but also for the perimeters of stronger shocks, since there β is near the value far upstream or downstream. We consider first the low pressure side of the shock, where β is near β_1. Upon introduction of

$$y = \beta_1 - \beta$$

and linearization also of the lefthand side of (18), we obtain as the solution of this linearized equation, which vanishes for $x \to -\infty$:

(19) $$y \sim \exp\left[-\frac{2\nu x}{UR_1^2} + x\left\{\left(\frac{2\nu}{UR_1^2}\right)^2 + 3\left(\frac{\beta_1-\beta_2}{R_1^2}\right)\right\}^{\frac{1}{2}}\right].$$

For

(20) $$\frac{2\nu}{UR_1} \gg (\beta_1-\beta_2)^{\frac{1}{2}},$$

this can be simplified to

$$y \sim \exp \frac{3Ux(\beta_1-\beta_2)}{4\nu},$$

which corresponds with the high pressure part of (16). Under most experimental conditions, however,

$$\frac{2\nu}{UR_1} \ll (\beta_1-\beta_2)^{\frac{1}{2}}, \tag{21}$$

in which case it follows that the front of te shock wave behaves as follows:

$$y \sim \exp - \left\{\frac{3(\beta_1-\beta_2)}{R_1^2}\right\} x. \tag{22}$$

For the high pressure side, β is near β_2. Then we write

$$\tilde{y} = \beta - \beta_2, \tag{23}$$

and linearize (18) with respect to β_2.

The solution for $\tilde{y}$, vanishing at $x \to \infty$ is

$$\tilde{y} \sim \exp\left[-\frac{2\nu x}{UR_2^2} + x\left\{\left(\frac{2\nu}{UR_2^2}\right)^2 - \frac{3(\beta_1-\beta_2)}{R_2^2}\right\}^{\frac{1}{2}}\right]. \tag{24}$$

When (20) holds, the solution is

$$y \sim \exp - \frac{3Ux(\beta_1-\beta_2)}{4\nu},$$

corresponding with the low pressure part of (16). When conditions are such that (21) is applicable, the solution is periodic, with wave length:

$$\lambda = \frac{2\pi R_2}{\{3(\beta_1-\beta_2)\}^{\frac{1}{2}}}. \tag{25}$$

The wave represented by this periodic solution is attenuated according to the factor $\exp -\frac{2\nu x}{UR_2^2}$.

With gravity waves on a free fluid surface, waves are known to appear under certain circumstances behind a hydraulic pump or bore (undular bore). The waves found here bear some resemblance to the waves associated with the undular bore. Apart from CHESTER's [7] theory, existing work on the undular bore deals only with the dispersive aspect, not in combination with dissipation by viscosity. Therefore, it cannot be said that the roles of viscosity in the mechanism of the undular bore and the shock wave described here are comparable. For both types of waves, it is clear that some dissipation is needed to make the existence of a steady shock or jump possible. The way in which viscosity affects the structure may be different in the two cases. As regards the waves, with wavelength given by (25), behind a shock wave in a liquid-bubble mixture, the following may be noted.

Pressure waves in such a mixture are dispersive, with a dispersion relation (see [3]) which may be written as:

$$k=\frac{\omega}{c\left\{1-\frac{\omega^2}{\omega_B^2}\right\}^{\frac{1}{2}}}. \tag{25}$$

Here ω and k are the angular frequency and the wave number, respectively, whereas c and ω_B are given by (2) and (14). No wave propagation is possible for ω near ω_B. From (14) it follows that behind the shock:

$$\omega_B=\frac{1}{R_2}\left(\frac{3p}{\rho_f}\right)^{\frac{1}{2}}.$$

The frequency associated with (25) is $2\pi U/\lambda$ or,

$$\frac{1}{R_2}\left\{\frac{3p_2\left(1-\frac{\beta_2}{\beta_1}\right)}{\rho_f}\right\}^{\frac{1}{2}}$$

Comparison shows that for strong shocks this is near ω_B behind the shock. In that case, the energy stored in resonance oscillations of the bubbles may play an important role in the mechanism of the shock wave. Also for weak shocks this mechanism may be of importance next to the mechanism described above. Noordzij and Van Wijngaarden [8] made some calculations on this aspect. The increase of the energy E^*, associated with resonance oscillations of the bubbles during the passage of a shock, can in the case of weak shocks be calculated by means of the theory of adiabatic invariants. It must be assumed that a bubble performs many resonant osscillations during the shock passage.
The theory of adiabatic invariants then results in the lowest approximation in

$$\frac{E^*}{\omega_B}=\text{constant}. \tag{26}$$

(In [8] this is carried further to higher approximations). (In the region 1 let the bubble perform oscillations with amplitude ε_1. Then calculating E^* and using (26), results in

$$E_2^*-E_1^*=\frac{15}{4}c_1^2\beta_1^2\frac{\varepsilon_1^2}{R_1^2}\left(\frac{p_2-p_1}{p_1}\right). \tag{27}$$

R_1 is the mean radius of the bubbles in front of the shock. On the other hand we may consider the regions far in front and behind the shock, assuming no bubble oscillations. For isothermal conditions and a steady state it follows that

$$(\tfrac{1}{2}u_2^2-\tfrac{1}{2}u_1^2)+\int_1^2\frac{dp}{\rho}=0. \tag{28}$$

The conservation of mass and momentum together with the assumption of an isothermal state, however, are sufficient to express the quantities behind the shock (subscript 2) in terms of the quantities in front of the shock (subscript 1). Carrying out the integration in (28) and using shock relations as, e.g., (1) and (7), it is found that in fact the left hand side of (28) is

(29) $$\frac{-c_1^2\beta_1^2}{3}\left(\frac{p_2-p_1}{p_1}\right)^3,$$

for weak shocks. Hence there is an apparent loss of energy across the shock. (A similar effect occurs with hydraulic jumps). When resonance oscillations are taken into account, this energy loss may be recovered in the increase of energy of the resonance oscillations. Comparison of (28) with (29) shows that a relative amplitude in the region 1

$$\frac{\varepsilon_1}{R_1}=0{,}3\left(\frac{p_2-p_1}{p_1}\right),$$

is sufficient to give rise to an increase in E^* of the absolute magnitude of (29).

EXPERIMENTS. Experiments on shock waves in bubble-liquid mixtures are being carried out by L. NOORDZIJ and H. G. RIKKERINK in our Laboratory. A detailed description of the apparatus etc. must be omitted here. We present only some preliminary results. Figure 2 and Fig. 3 show shock waves in a bubble-liquid mixture. The values of the pertinent parameters are

	$\frac{p_1}{p_2}$	R_1	β_1	d
Fig. 2	0·46	$1{\cdot}25\times10^{-3}$	$2{\cdot}86\times10^{-2}$	$6{\cdot}1\times10^{-2}$
Fig. 3	0·27	$1{\cdot}50\times10^{-3}$	$4{\cdot}95\times10^{-2}$	$3{\cdot}7\times10^{-2}$.

Figure 4 shows the pressure recording associated with the shock of Fig. 2. Clearly visible are the waves behind the shock as predicted by the theory. According to the theory given here, the width of the front part of the shock is of order $\frac{R_1}{(\beta_1-\beta_2)^{\frac{1}{2}}}$ (cf. Eq. 22). According to the present theory, the shock thickness d is therefore of order $\frac{R_1}{(\beta_1-\beta_2)^{\frac{1}{2}}}$.

(30) $$d\sim\frac{R_1}{\beta^{\frac{1}{2}}\left(1-\frac{p_1}{p_2}\right)^{\frac{1}{2}}}.$$

For a number of experiments including those of Fig. 2 and Fig. 3, the parameter $\frac{d\beta_1^{\frac{1}{2}}}{R_1}$ was therefore plotted against the ratio p_1/p_2, resulting in Fig. 5 It was found that the curve

(31) $$d=\frac{4{\cdot}8R_1}{\beta_1^{\frac{1}{2}}\left(1-\frac{p_1}{p_2}\right)^{\frac{1}{2}}},$$

is a reasonable representation of the experimental data. This curve is, together with the experimental data, shown in Fig. 5. The maximum relative deviation from this curve

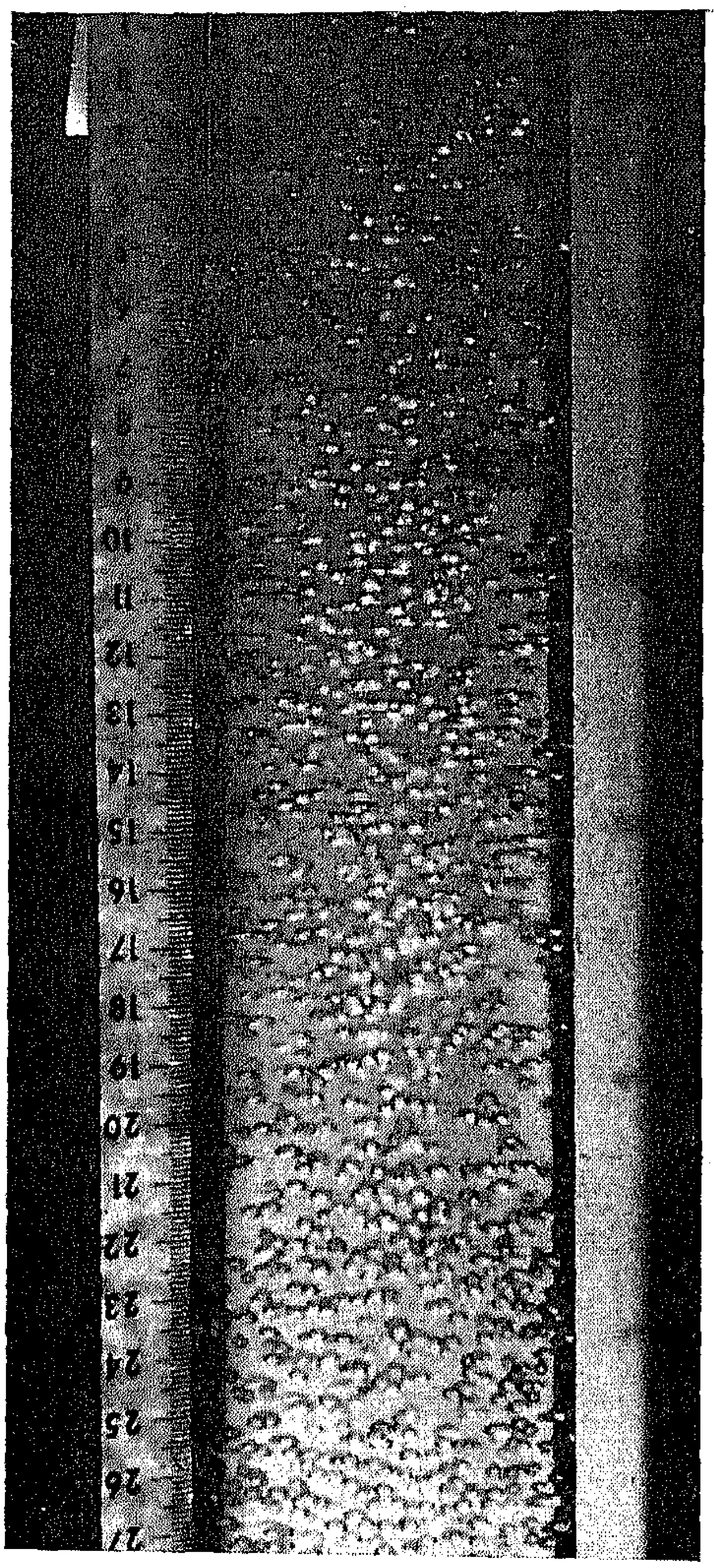

FIG. 2. Shock wave propagating downwards through bubble-liquid mixture. The high pressure side is on the top of the picture. The shock is between the numbers (photographed upside down) 20 and 14. Values of bubble size etc. are given in text.

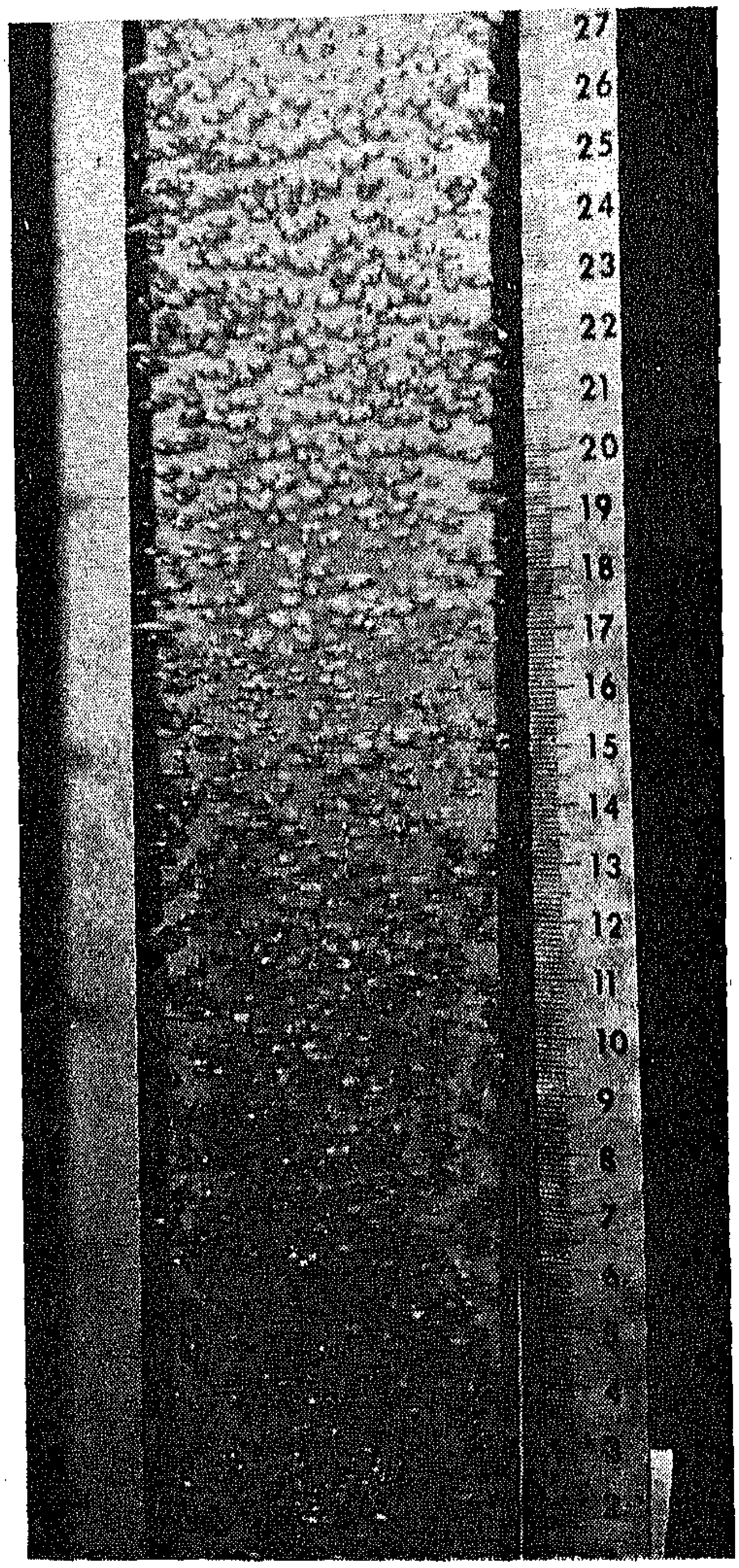

FIG. 3. Idem. Shock wave is between numbers 20 and 16.

is less than 20%. In view of the fact that the accuracy with which the bubble size R can be measured is also about 20%, a reasonable agreement with theory can be noticed.

Another comparison of theory and experiment can be made by considering the wavelength in Fig. 4. According to theory, this has the value (cf. (25)):

$$\frac{2\pi R_2}{\left\{3\beta_1\left(1-\frac{p_1}{p_2}\right)\right\}^{\frac{1}{2}}} \quad \text{or} \quad = \frac{2\pi R_1\left(\frac{p_1}{p_2}\right)^{\frac{1}{3}}}{\left\{3\beta_1\left(1-\frac{p_1}{p_2}\right)\right\}^{\frac{1}{2}}}.$$

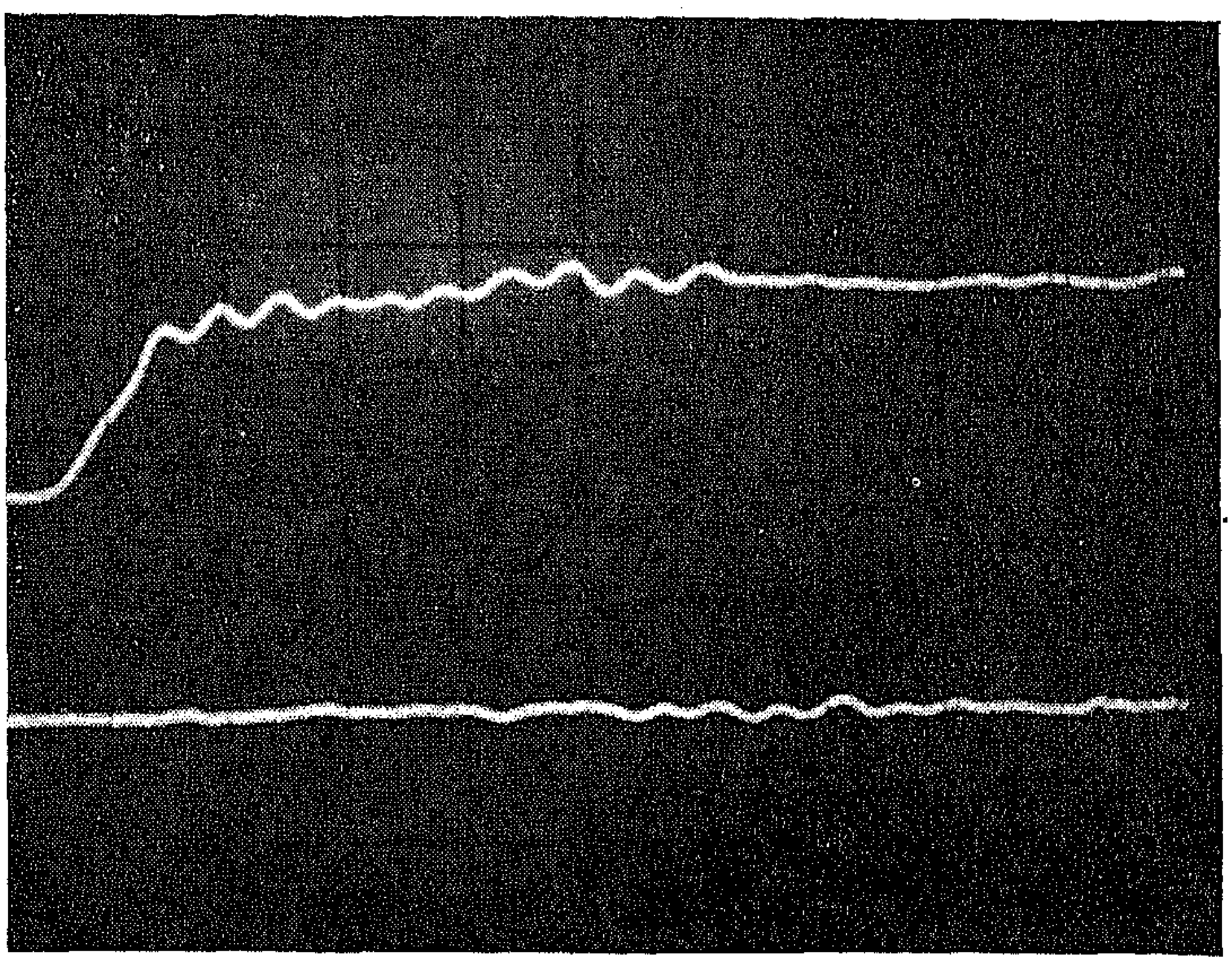

FIG. 4. (Only upper curve applies). Recording of pressure across shock wave in bubble-liquid mixture, as shown in Fig. 2. Clearly visible are the waves behind the shock.

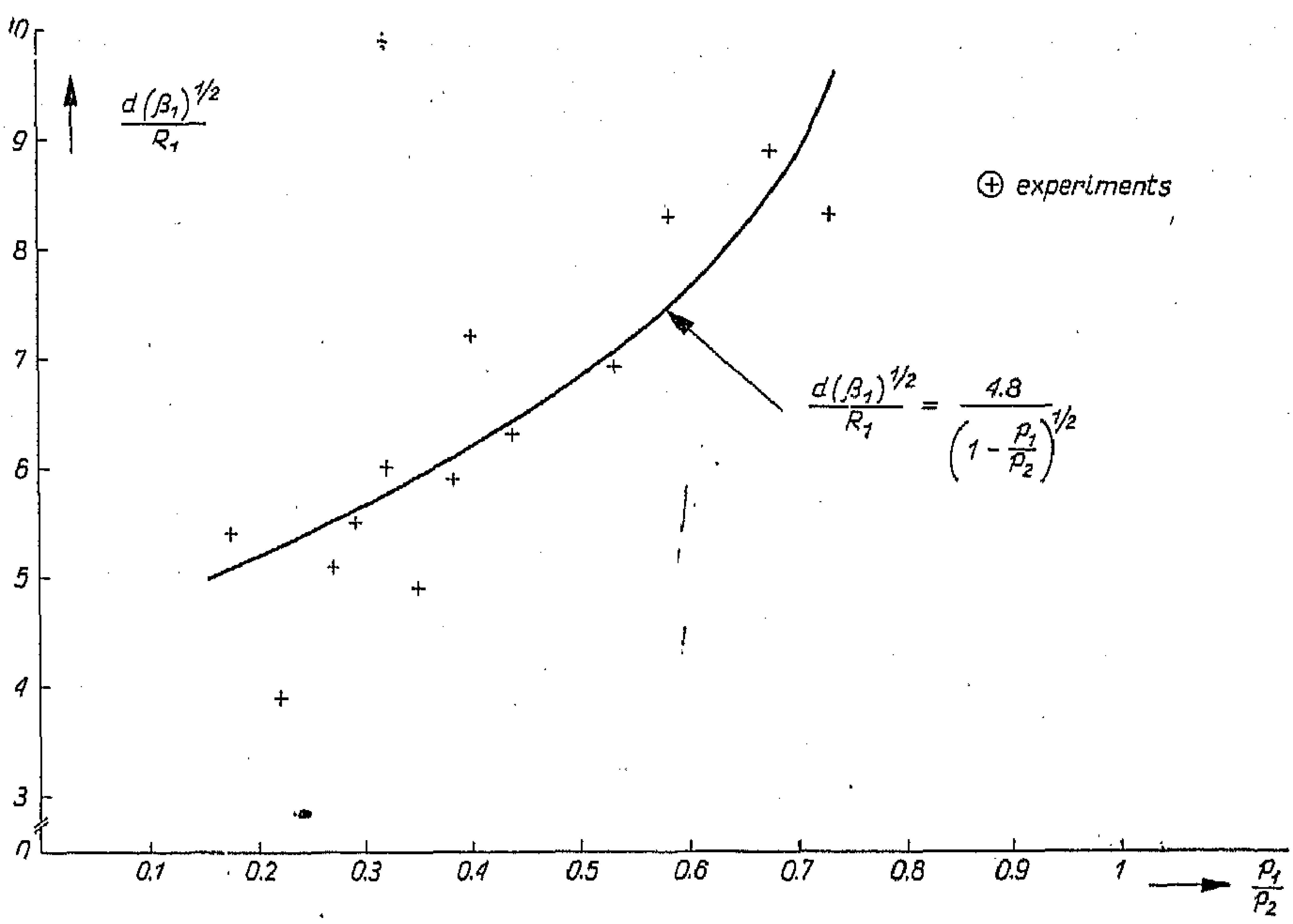

FIG. 5. Diagram showing the dimensionless shock thickness $\frac{d\beta_1^{\frac{1}{2}}}{R_1}$ as a function of the pressure ratio p_1/p_2. The solid curve follows, up to the numerical constant, from the theory.

Comparison with Eq. (31) gives $\frac{\lambda}{d}=0.7\left(\frac{p_1}{p_2}\right)^{\frac{1}{3}}$. For the experiment of Fig. 4, $\frac{p_1}{p_2}=0.46$, and therefore this gives $\lambda=0.6\,d$.

From Fig. 5 it follows that experimentally this ratio is 0.7, which is in satisfactory agreement with the theoretical value.

In conclusion, we may say that the preliminary measurements reported here give encouraging support to the theory which predicts shock waves with a thickness given by (30) accompanied by pressure waves at the rear side with wavelength given by (25).

References

[1] L. van Wijngaarden, *The structure of shock waves in liquid-bubble mixtures*, Phys. Comm. Twente Institute of Technology, **1**, **2**, 1969.

[2] I. J. Campbell, A. S. Pitcher, *Shock waves in liquid containing gas bubbles*, ARL report RE/G/HY//17/0, 1957.

[3] L. van Wijngaarden, *On the equations of motion for mixtures of liquid and gas bubbles*, J. Fluid Mech., **33**, **3**, 465, 1968.

[4] G. K. Batchelor, *Compression waves in a suspension of gas bubbles in liquid*, Fluid Dynamics Transactions, vol. **4**, 425 - 447, 1969.

[5] L. D. Landau, E. M. Lifshitz, *Fluid Mechanics*, Pergamon Press, 1959.

[6] H. Lamb, *Hydrodynamics*, Cambridge University Press, 1932.

[7] W. A. Chester, *A model for the undular bore on a viscous fluid*, J. Fluid Mech., **24**, 2, 367, 1966.

[8] L. Noordzij, L. van Wijngaarden, to be published.

TWENTE INSTITUTE OF TECHNOLOGY THE NETHERLANDS